The role of lanthanum oxide on Pd-only three-way catalysts prepared by co-impregnation and sequential impregnation methods

Do Heui Kim [a], Seong Ihl Woo [a,*], Jin Man Lee [b] and O-Bong Yang [b]

[a] *Department of Chemical Engineering, Korea Advanced Institute of Science and Technology, Taejon 305-701, Korea*
E-mail: siwoo@mail.kaist.ac.kr
[b] *School of Chemical Engineering and Technology, Chonbuk National University, Chonju, Chonbuk 561-756, Korea*

Received 22 March 2000; accepted 20 September 2000

The effect of lanthanum oxides on the catalytic performance and the physicochemical properties of Pd-only three-way catalysts prepared by co-impregnation and sequential impregnation methods was studied by using hydrogen chemisorption, BET surface area, X-ray diffraction and X-ray photoelectron spectroscopy. It was found that the roles of La closely depended on the order of La introduction in the preparation of the Pd catalysts. Pd–La/Al_2O_3 prepared by co-impregnation of La and Pd, kept its superior activity in spite of the significant loss of surface area of the alumina support after thermal aging at 1273 K, indicating that the primary role of La was a Pd stabilizer through the intimate interaction between La and Pd. However, on Pd/La/Al_2O_3, in which Pd was consecutively impregnated after the impregnation of La, La preferentially interacted with the alumina support as a form of $La_xAl_yO_2$, resulting in the stabilization of the alumina support during thermal aging. XPS results indicated that lanthanum oxide suppressed the formation of PdO interacting with alumina during thermal aging. In the case of Pd/La–Ce/Al_2O_3, the formation of the solid solution of $(Ce_xLa_{1-x})O_2$ was not strong enough to maintain the high activity and the good textural property after thermal aging.

Keywords: Pd-only three-way catalyst, lanthanum oxide, cerium oxide, co-impregnation, XPS, XRD, thermal aging

1. Introduction

Palladium as an active metal in a three-way catalyst (TWC) has been known to have a good resistance to thermal sintering, a lower price than Rh and a higher activity for the oxidation of hydrocarbons and CO [1]. Pd-only TWC has been intensively studied as a new generation three-way catalyst even in applications where catalyst temperature occasionally reaches 1273 K [2]. However, Pd-only TWC shows a relatively low activity for the NO removal in oxygen-rich conditions. It is well known that the Rh component in the conventional Pt/Rh catalyst is responsible for that role [3]. Lanthanide oxides such as La and Ce [4], and base metal oxides such as Co, Ba and Zr [5–8] have been used as promoters to improve the catalytic activity of Pd-only TWC. Especially La_2O_3 is known to act as a good promoter to increase the dispersion and the thermal stability [9], and improve the oxidation activity of Pd [10]. In addition, CeO_2 plays an important role as an oxygen storage capacitor (OSC) which stores the oxygen during lean conditions and releases it during rich conditions [11], provides the activity for water–gas shift reaction [12], maintains the dispersion of the catalytic active metals [13,14], and stabilizes the surface area of the alumina washcoat [15,16].

There are a few reports on the interaction between Al_2O_3 and the lanthanide oxides. Shyu et al. [17] reported that the reaction between CeO_2 and Al_2O_3 which transformed CeO_2 into other more stable compounds, $CeAlO_3$, under high temperature reducing conditions was expected to adversely affect the OSC by fixing one oxidation state. To avoid such effects, La^{3+} as an Al_2O_3 modifier was introduced to block the reaction between Al_2O_3 and CeO_2. Graham et al. [18] postulated that $CeO_2/La_2O_3/Al_2O_3$ showed a higher CeO_2 dispersion and a greater OSC of the CeO_2 than co-impregnated $(CeO_2 + La_2O_3)/Al_2O_3$ and $La_2O_3/CeO_2/Al_2O_3$ from the XPS results. Shelef et al. [19] showed in a model catalyst study that the presence of lanthanum oxide in the films inhibited the reduction of cerium oxide partially. In practice, the thermal stability of the TWC is very important for its commercial application. The physicochemical properties of lanthanum-modified Al_2O_3 as a function of the amount of La were investigated by XPS and CO_2 absorption [20]. As a result, a consequence of the high calcination temperature of 925 °C facilitated the diffusion of surface lanthanum into the alumina bulk to form $LaAlO_3$. Likewise, the roles of La have been focused on the enhanced thermal stability of the Al_2O_3 support or the increased OSC of the catalyst containing cerium oxide.

Co-impregnation has been known as a catalyst preparation method with a view to forming bimetallic particles [21]. Although co-impregnated Pd–Pt [21] and Pd–Rh [22] catalysts were reported for hydrocarbon oxidation and NO reduction, respectively, there is, to our knowledge, no result about the co-impregnation effect of Pd and La in the three-way catalytic reaction. Since the strong metal–support interaction is well known in Pd/La_2O_3 [23], an intimate interaction of Pd and lanthanum oxide arising from co-impregnation is expected to result in a catalyst with a novel activity. In this work, the role and the effect of La

---

[*] To whom correspondence should be addressed.

and Ce oxides on the catalytic performance and the physicochemical properties of Pd-only TWC as a function of impregnation mode were investigated by three-way catalytic reaction, X-ray photoelectron spectroscopy (XPS), X-ray diffraction (XRD), BET and hydrogen chemisorption. To elucidate the role of lanthanum oxide, the physicochemical properties of a co-impregnated Pd–La/Al_2O_3 and a successively loaded Pd/La/Al_2O_3 were compared.

2. Experimental

2.1. Catalyst preparation

All the catalysts were prepared by a wet impregnation method. The γ-Al_2O_3 support (Nishio Co., Japan) has a packed density of 0.60 g/cm^3, BET surface area of 160 m^2/g and particle size of 20–70 mesh. Nitrate forms of Pd, Ce and La were used as precursors. The metal loadings of Pd, La and Ce are 1, 3 and 5 wt%, respectively, if the number in the bracket is not described. After impregnation of La or/and Ce precursors on γ-Al_2O_3 followed by drying and calcination, Pd was consecutively impregnated for the preparation of promoted catalysts denoted as Pd/La/Al_2O_3, Pd/Ce/Al_2O_3 and Pd/Ce–La/Al_2O_3. In comparison with Pd/La/Al_2O_3, the catalyst designated as Pd–La/Al_2O_3 was prepared by co-impregnation of La and Pd precursor simultaneously. All the catalysts calcined at 873 K with air stream for 3 h were called as “fresh” catalyst. In addition, “aged” catalyst was obtained by treating the fresh catalyst at 1273 K with air stream for 10 h.

2.2. Three-way catalytic performance test

The three-way catalytic reaction was carried out at stoichiometric air/fuel ratio (14.7) and gas hourly space velocity of 72 000 h^{-1} (400 cm^3/min) in a continuous U-tube quartz reactor with simulated exhaust gas containing 6000 ppm CO, 1500 ppm NO, 500 ppm C_3H_6, 3000 ppm H_2, 6000 ppm O_2 and 13% H_2O in N_2 balance. The reactant and product gases were analyzed by a gas chromatograph (DS6200, DONAM Systems, Korea) equipped with a thermal conductivity detector for CO and a flame ionization detector for C_3H_6, and by a chemiluminescence NO_x analyzer (42H, Thermo Environmental Instruments, Inc., USA). The reaction data were measured at a desired temperature after treating the catalyst with air stream at 773 K.

2.3. Catalyst characterization

BET surface area of a catalyst was obtained from the nitrogen adsorption isotherm at 77 K in a Micromeritics ASAP 2010C analyzer. Before the measurements, all the samples were degassed to 10^{-4} Torr. For the hydrogen chemisorption, the total and reversible adsorption isotherms of hydrogen were obtained with a sample of 0.3 g at 373 K after degassing the pre-adsorbed hydrogen at 673 K and 1×10^{-5} Torr for 2 h in the same apparatus. The difference between total and reversible adsorption isotherm corresponded to the amount of hydrogen atoms chemisorbed irreversibly and reported herein. XRD experiment was performed with the target of Cu Kα ($\lambda = 1.540598$ Å) operated at 40 kV and 45 mA with a scan speed of 4°/min. XPS spectra were taken in a surface analysis chamber (LHS-10; SPECS GmbH, Germany). X-ray (Al Kα, 1486.6 eV) radiated at a power of 300 W (30 mA, 10 kV). The kinetic energy of an ejected electron was analyzed by a multiple channel detector in a hemispherical energy analyzer. The pass energy was 98 eV and the base pressure of the analysis chamber was 8×10^{-10} Torr. Energy shifts of binding energy occurred due to the electron charging effect. Each spectrum was calibrated using the peak of C 1s (284.6 eV) as a standard. The accuracy of the spectrum was ±0.2 eV. Data smoothing, subtraction of background (Shirley method), and the curve fitting (Voigt ratio 30) were taken with SPECTRA software from SPECS GmbH. The relative atomic sensitivity factor (La 3d: 9.122, Ce 3d: 8.808, Al 2p: 0.234, Pd 3d: 5.356) was obtained from [24].

3. Results

3.1. Three-way catalytic performance test

Table 1 shows the light-off temperature in which the conversion reaches 50% (T_{50}, °C) for NO, CO and C_3H_6 on various catalysts. Since the emission regulations such

Table 1

T_{50} (K) and T_{50} difference (Δ) between fresh and aged catalysts for the removal of NO, CO and C_3H_6.

		Pd/Al_2O_3	Pd/La/Al_2O_3	Pd/Ce/Al_2O_3	Pd/La–Ce/Al_2O_3	Pd–La/Al_2O_3	Pd/Ce(30)/Al_2O_3
NO	Fresh	579	583	565	510	565	529
	Aged	635	603	605	586	583	616
	Δ	56	20	40	76	18	87
CO	Fresh	580	573	485	461	546	453
	Aged	584	633	485	496	491	488
	Δ	4	60	0	35	−55	35
C_3H_6	Fresh	578	573	553	544	554	523
	Aged	606	593	584	594	577	605
	Δ	28	20	31	50	23	82

as LEV II standards in California will strictly limit NO_x other than CO or hydrocarbons, we focus on the light-off temperature for NO. Both fresh and aged Pd/Al_2O_3 reveal the highest T_{50} for all of the reactants. However, the T_{50} of fresh La- and/or Ce-promoted catalysts, whatever the loading and preparation methods, is significantly lower than that of Pd/Al_2O_3. The T_{50} differences (Δ) between fresh and aged catalysts containing La, $Pd/La/Al_2O_3$ and $Pd–La/Al_2O_3$, are smallest among the catalysts, indicating its excellent thermal stability under aging. Especially T_{50} of aged $Pd–La/Al_2O_3$ is much lower than that of $Pd/La/Al_2O_3$. This result indicates that the catalytic activity and the thermal stability are affected by the order of introducing La and Pd during the preparation of the catalysts. The promoter effect of La on the catalytic activity is significantly increased on $Pd–La/Al_2O_3$.

Although fresh $Pd/Ce(30)/Al_2O_3$ shows the lowest T_{50} among fresh ones, the T_{50} is drastically increased upon aging. While the fresh $Pd/Ce(30)/Al_2O_3$ shows lower T_{50} than that of fresh $Pd/Ce/Al_2O_3$, the T_{50} of aged one is much higher than that of aged $Pd/Ce/Al_2O_3$ one. It means that the catalyst containing Ce which is an activity enhancing promoter is largely deactivated on aging. In the case of $Pd/La–Ce/Al_2O_3$, the advantageous effect of lanthanum oxide on the enhancement of the thermal stability disappears from the large $T_{50,NO}$ difference of 76 K. In other words, the addition of La cannot maintain the high activity of fresh $Pd/La–Ce/Al_2O_3$.

3.2. Surface area and hydrogen chemisorption

The surface areas of all catalysts are definitely decreased on aging, as shown in table 2. $Pd/La/Al_2O_3$ shows the highest surface area among the aged catalysts. However, the surface area of the aged $Pd/Ce/Al_2O_3$ is considerably decreased, whereas that of $Pd/La–Ce/Al_2O_3$ is not largely decreased on aging. The surface areas of the fresh $Pd/La/Al_2O_3$ and the fresh $Pd–La/Al_2O_3$ are similar, but the aged $Pd/La/Al_2O_3$ has a higher surface area than the aged $Pd–La/Al_2O_3$, which also implies the formation of different textural structure on two catalysts after thermal aging.

The Pd dispersion of a fresh $Pd/La–Ce/Al_2O_3$ is the highest according to the hydrogen chemisorption data in table 3. However, its dispersion is extremely decreased after aging. Although the fresh $Pd/La/Al_2O_3$ has relatively low dispersion of 12.33%, the aged one retains the highest dispersion among the aged catalysts. Although the Pd dispersions in the fresh $Pd–La/Al_2O_3$ and $Pd/La/Al_2O_3$ are quite similar, the dispersion of the aged $Pd–La/Al_2O_3$ is drastically decreased due to the significant thermal sintering. The effect of La on the retention of high dispersion during thermal aging is not great on $Pd–La/Al_2O_3$ and $Pd/La–Ce/Al_2O_3$. The BET surface area and hydrogen chemisorption data clearly indicate that lanthanum oxides play a crucial role in maintaining the high surface area of alumina and the dispersion of Pd, especially in case of sequentially loaded $Pd/La/Al_2O_3$ catalyst under the thermal aging with O_2 at 1273 K.

3.3. XRD

Figure 1 shows the XRD patterns of the fresh catalysts. Major peaks correspond to γ-Al_2O_3 and CeO_2 phases. Only $Pd/La/Al_2O_3$ contains the broad PdO phase (figure 1(b)). Peak patterns of $Pd/Ce/Al_2O_3$ and $Pd/Ce–La/Al_2O_3$ are almost the same. In other words, no lanthanum related peaks are detected on a $Pd/La/Al_2O_3$ containing 1.27 μmol-La/m^2. This is in good agreement with the previous result that the

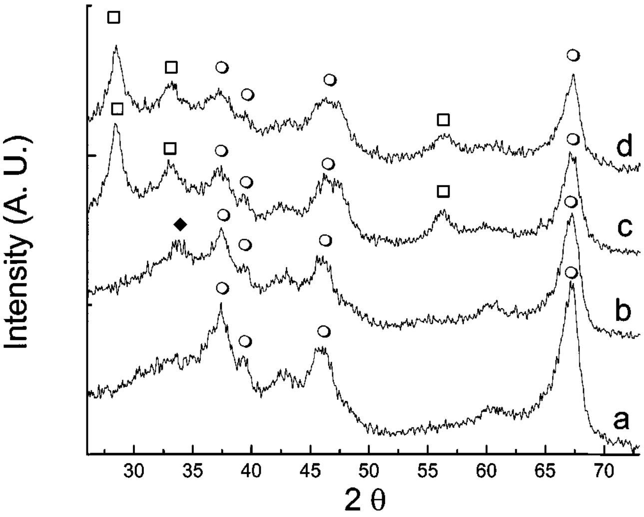

Figure 1. XRD patterns of fresh catalysts: (a) Pd/Al_2O_3, (b) $Pd/La/Al_2O_3$, (c) $Pd/Ce/Al_2O_3$ and (d) $Pd/La–Ce/Al_2O_3$. (○) γ-Al_2O_3, (◆) PdO and (□) CeO_2.

Table 2
BET surface areas (m^2/g) of various catalysts.

	Pd/Al_2O_3	$Pd/La/Al_2O_3$	$Pd–La/Al_2O_3$	$Pd/Ce/Al_2O_3$	$Pd/La–Ce/Al_2O_3$
Fresh	164.88	163.82	163.20	154.79	156.83
Aged	89.93	108.60	96.01	85.92	93.02

Table 3
Dispersion (%) of Pd by hydrogen chemisorption.

	Pd/Al_2O_3	$Pd/Ce/Al_2O_3$	$Pd/La/Al_2O_3$	$Pd–La/Al_2O_3$	$Pd/La–Ce/Al_2O_3$
Fresh	28.73	27.54	12.33	10.82	35.49
Aged	4.10	4.02	7.07	2.33	1.14

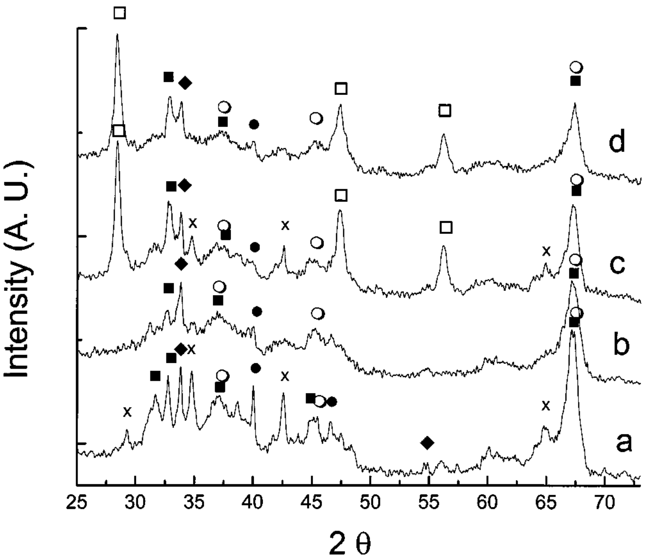

Figure 2. XRD patterns of aged catalysts: (a) Pd/Al_2O_3, (b) $Pd/La/Al_2O_3$, (c) $Pd/Ce/Al_2O_3$ and (d) $Pd/La–Ce/Al_2O_3$. (○) γ-Al_2O_3, (◆) PdO, (□) CeO_2, (■) θ-Al_2O_3, (●) Pd and (×) κ-Al_2O_3.

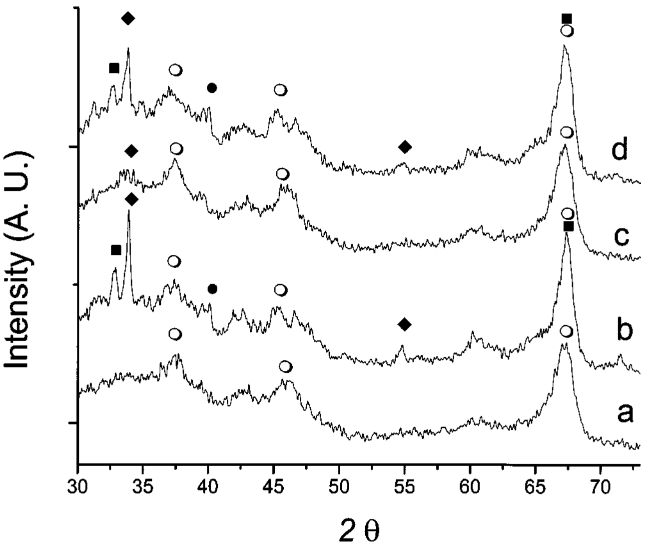

Figure 3. XRD patterns of the catalysts containing lanthanum oxide: (a) $Pd–La/Al_2O_3$ fresh, (b) $Pd–La/Al_2O_3$ aged, (c) $Pd/La/Al_2O_3$ fresh and (d) $Pd/La/Al_2O_3$ aged. (○) γ-Al_2O_3, (◆) PdO, (■) θ-Al_2O_3 and (●) Pd.

lanthana up to 8.5 μmol-La/m^2 exist in the form of a two-dimensional overlayer on the alumina support invisible by XRD [25].

After aging the catalysts, the peaks grow sharper and the new peaks such as metallic Pd, θ-Al_2O_3 and κ-Al_2O_3 come out, as shown in figure 2. Especially the growth of Pd metallic phase is noticeable in Pd/Al_2O_3. Most Al_2O_3 phases are θ-Al_2O_3 and κ-Al_2O_3 on an aged Pd/Al_2O_3. The addition of La and/or Ce oxides gives rise to the inhibition of the phase transition of γ-Al_2O_3 (figure 2 (b), (c) and (d)) to θ-Al_2O_3 and κ-Al_2O_3. Like the fresh $Pd/La/Al_2O_3$, no peaks concerning the La species such as La_2O_3 or $LaAlO_3$ are found in the other catalysts containing lanthanum oxide even after aging, because the two-dimensional La_2O_3 invisible by XRD does not act as a precursor to the formation of $LaAlO_3$ [26]. γ-Al_2O_3 phase is maintained only on aged $Pd/La/Al_2O_3$, resulting in the high surface area, as shown in table 2. Figure 3 shows the XRD patterns of La-promoted Pd/Al_2O_3. In comparison with aged $Pd/La/Al_2O_3$ (figure 3(d)), the peaks of PdO ($2\theta = 33.8°$) and θ-Al_2O_3 ($2\theta = 32.8°$) phases on aged $Pd–La/Al_2O_3$ (figure 3(b)) are obviously increased, which indicates that the sintering of Pd species and the phase transformation of γ-Al_2O_3 to θ-Al_2O_3 much more proceeded on a $Pd–La/Al_2O_3$ than on a $Pd/La/Al_2O_3$. These distinct textural properties after thermal aging seem to be due to the different role of La in two catalysts.

The drastic growth of the CeO_2 phase on a Ce-promoted catalyst shows a negative effect on the oxygen storage capacity which depends on CeO_2 crystalline structure [27]. The advantageous effect of La on the inhibition of phase transformation of Al_2O_3 is not so large on $Pd/La–Ce/Al_2O_3$. The change in the lattice constant of CeO_2 in the $Pd/La–Ce/Al_2O_3$ is estimated from the shifts of a peak at $2\theta = 56.38°$, arising from $CeO_2(311)$ plane [28]. The 2θ of the fresh $Pd/La–Ce/Al_2O_3$ is 56.36° corresponding to that of pure CeO_2, which indicates that La–Ce solid solution is not formed. It changes to 56.20° on aging, which means that La^{3+} ions are dissolved into the CeO_2 lattice during the thermal aging, since the radius of the La^{3+} ion (1.19 Å) is larger than that of the Ce^{4+} ion (1.09 Å). The formation of La–Ce solid solution as shown in the XRD pattern by the dissolution of La^{3+} ions into CeO_2 lattice has been known as the key process in maintaining the good oxygen storage capacitor under the thermal treatment [18]. However, it is unsatisfactory to maintain the good activity and the textural property of fresh $Pd/La–Ce/Al_2O_3$ after the thermal aging according to the results of reaction performance and BET surface area.

3.4. XPS

XPS data of various Pd catalysts are summarized in table 4. When the catalysts are aged, Pd $3d_{5/2}$ peak areas become smaller, meaning that Pd surface concentration is decreased due to the thermal sintering. Such XPS results are consistent with the result of hydrogen chemisorption, as shown in table 3. Binding energy of Pd $3d_{5/2}$ in Pd/Al_2O_3 is 336.7 eV, which can be assigned to PdO by the previous XPS data [26,29]. Binding energies of Pd $3d_{5/2}$ in fresh La- and/or Ce-promoted catalysts are lower than that of Pd/Al_2O_3 by 0.5–0.7 eV, indicating the formation of less oxidized PdO_{1-x} species. After aging the Pd/Al_2O_3, the binding energy of Pd $3d_{5/2}$ shifts to 336.2 eV which is assigned to that of PdO_{1-x} species. A small shoulder appears at 338.4 eV which can be assigned as the binding energy of PdO_2 or deficiently coordinated Pd^{2+} [29]. However, the latter one seems to be more probable than the former one because PdO_2 exists only in the hydrous form [30]. As the Pd/Al_2O_3 is aged, the PdO is either reduced to the less oxidized PdO_{1-x} or diffused to the boundary site of

Table 4
Binding energy of Pd $3d_{5/2}$ and the relative surface concentration of Pd/Al.

		BE (eV)	Pd/Al (×100)
Pd/Al_2O_3	Fresh	336.7	0.50
	Aged	336.2	0.09
		338.4	0.06
$Pd/La/Al_2O_3$	Fresh	336.0	0.51
	Aged	336.2	0.19
$Pd/Ce/Al_2O_3$	Fresh	336.0	0.52
	Aged	336.8	0.18
$Pd/La–Ce/Al_2O_3$	Fresh	336.2	0.51
	Aged	336.6	0.23
$Pd–La/Al_2O_3$	Fresh	336.2	1.68
	Aged	335.5	0.42

Al_2O_3 thus to PdO interacting with Al_2O_3 having higher binding energy. Farrauto [31] suggested that the bulk-like PdO species was much more active than the PdO interacting with Al_2O_3 species in methane combustion. The addition of lanthanide oxides suppresses the formation of such PdO species on the aged catalysts (table 4) possibly by blocking the diffusion of PdO to alumina, thus resulting in the superior reactivity of the aged catalysts containing lanthanide oxide (table 1). It was described in section 3.3 that the aged $Pd–La/Al_2O_3$ showed a better activity than that of aged $Pd/La/Al_2O_3$ in spite of the lower surface area and the higher degree of crystallinity, which could be well explained by XPS data that the Pd surface concentration of the former one was more than three times larger than that of the latter one.

When $Pd–La/Al_2O_3$ is aged, the binding energy of Pd is shifted to more metal-like PdO_{1-x} species (335.5 eV). The binding energy shifts on the insulator support are influenced not only by the chemical state of the metal, but also by the final state effect arising from the size of the supported metal crystallites. However, the effects of particle size are negligible, if the supported metal particles are large enough to exhibit bulk-like valence structure. The dispersion of the samples studied here ranges between 1 and 36%, as shown in table 3. The minimum estimated average diameter of the Pd particles was 5 nm, based on the equation suggested by Bell [23]. According to the review paper by Karpinski [32], Pd particles larger than 4 nm were treated as bulk Pd. Therefore, the final state effects arising from the particle size of Pd can be excluded.

Accordingly the binding energy shift is attributed to the charge transfer from LaO_x to Pd [33], arising from the intimate interaction between Pd and La on the surface during the thermal aging. On the other hand, the thermal aging on the sequentially loaded catalyst, $Pd/La/Al_2O_3$, does not affect the electronic environment of Pd, resulting in the similar binding energy of Pd 3d to that of fresh $Pd/La/Al_2O_3$. It can be explained by relatively weak interaction between Pd and La on $Pd/La/Al_2O_3$ in comparison with that on $Pd–La/Al_2O_3$. Table 5 shows the binding energy of La $3d_{5/2}$ and the relative surface concentration of La/Al for the La-loaded catalysts. The binding energies of 833.5 and 835 eV are assigned to La $3d_{5/2}$ of pure La_2O_3 oxides and that of dispersed La_2O_3 phase, respectively [34]. Therefore, the La species on our catalysts possibly correspond to the latter one. Furthermore, the binding energy of La $3d_{5/2}$ of all La-loaded catalysts was not changed on thermal aging. In summary, the interaction between Pd and La is significant on the catalyst prepared by co-impregnating both of these, resulting in the surface-abundance of Pd and La, the improved thermal stability of Pd and the enhanced catalytic activity.

Table 5
Binding energy of La $3d_{5/2}$ and the relative surface concentration of La/Al.

		BE (eV)	La/Al (×100)
$Pd/La/Al_2O_3$	Fresh	835.8	1.82
	Aged	835.6	2.28
$Pd–La/Al_2O_3$	Fresh	835.4	3.25
	Aged	835.6	4.65
$Pd/La–Ce/Al_2O_3$	Fresh	835.7	1.40
	Aged	835.7	2.33

4. Discussion

La_2O_3 has been well known as a promoter to have a good thermal resistance. In this study, it was also confirmed that Ce and La are promoters for the catalytic activity and thermal stability, respectively. It is notable that the role of La on the Pd-only three-way catalyst is significantly affected by the impregnating order of La and Pd on γ-Al_2O_3 support. On $Pd/La/Al_2O_3$, La_2O_3 played a crucial role of inhibiting the phase transformation from γ-Al_2O_3 to θ-Al_2O_3, resulting in the maintenance of the high surface area after thermal aging. Capitan et al. [34] ascribed it to the strong interaction between La cation and the support, which resulted in a redistribution of the electronic density over Al–O–La ensembles from the spectroscopic measurements and *ab initio* calculations. On the other hand, on $Pd–La/Al_2O_3$, the intimate interaction between lanthanum oxide and Pd was a primary observation. A high surface concentration of Pd and a charge transfer from LaO_x to Pd, as shown in table 4, seemed to arise from the intimate interaction of lanthanum oxide with Pd. Therefore, the degree of interaction with Pd closely depended on the order of the addition of La during catalyst preparation. First, the major function of La on $Pd/La/Al_2O_3$ was the suppression of a thermal sintering of alumina texture through an interaction between La and Al like a La–O–Al bond which might be formed during the calcination of La/Al_2O_3 before impregnation of Pd. However, there was no significant effect of La on the electronic structure of Pd species in this case in comparison of XPS data with that of $Pd–La/Al_2O_3$. Second, the La on Pd–La/Al_2O_3 played a main role as a promoter to enhance the thermal stability of Pd through an intimate interaction between Pd and La possibly as a form of Pd–La ensemble which seemed to be formed by the calcination of Pl–La/Al_2O_3. The higher surface concentration of Pd/Al on Pd–La/Al_2O_3 than that on Pd/La/Al_2O_3 was interesting, because Pd was finally loaded on the latter one. It could be explained by the intimate interaction between Pd and La that might be maintained on the surface during thermal aging, thus resulting in the higher surface concentration of Pd/Al and La/Al as shown in XPS. In addition, the intimate contact of Pd and La on Pd–La/Al_2O_3 might give rise to the easy charge transfer from LaO_x to Pd to form rather electron-rich PdO_{1-x} species.

Two types of PdO species were reported in the Pd catalysts supported on Al_2O_3 by Farrauto et al. [31]. One is easily reducible PdO covering Pd metal particles, which is reduced to metallic Pd in H_2 even at RT, and this PdO species have the similar binding energy to bulk PdO by XPS study [29]. The other is a stable palladium oxide strongly interacting with alumina. TPO/TPR study showed that the ratio of O to Pd was more than one, in other words, oxygen rich, and that it was reduced at higher temperature [10]. In methane combustion, the former PdO species (PdO covering metal particles) were suggested to be much more active than the latter one (PdO interacting with Al_2O_3). The binding energy of Pd $3d_{5/2}$ in aged Pd/Al_2O_3 (338.4 1eV) was higher than that of bulk PdO (336.7 eV) by 1.7 eV, as shown in table 4. It was demonstrated that the presence of lanthanide oxides suppressed the formation of PdO interacting with Al_2O_3 during thermal aging from the result of XPS. By analogy to the methane combustion, the absence of PdO interacting with Al_2O_3 on Pd/Al_2O_3 containing lanthanide oxide accounts for the higher three-way catalytic activity than Pd/Al_2O_3 after thermal aging.

In spite of the formation of the solid solution of $(Ce_xLa_{1-x})O_2$ on Pd/La–Ce/Al_2O_3, as shown figure 2, Pd/La–Ce/Al_2O_3 was rapidly deactivated upon aging. In other words, when La was co-impregnated with Ce, its thermal stabilizing effect was not observed. Therefore, an alternative method must be found to keep the excellent property of each promoter, La and Ce. To achieve the optimum performance of Pd-only three way catalyst, it was shown that ceria had to be separated from the Pd active species or promoters by physical mixing in our recent results [35].

5. Conclusions

The role of La significantly depended on the impregnating order of La and Pd on the Pd-only three-way catalyst supported on alumina. When La was co-impregnated with Pd on Pd–La/Al_2O_3, which showed a high activity, the major role of La was a promoter to enhance the thermal stability of Pd through an intimate interaction between Pd and La, resulting in the electron-rich PdO_{1-x} species. However, La predominantly interacted with alumina and played as a promoter to suppress a thermal sintering of alumina texture on Pd/La/Al_2O_3 that was prepared by loading La first and then introducing Pd serially. In the case of Pd/La–Ce/Al_2O_3, the formation of La and Ce oxides solid solution was not strong enough to maintain the high activity and the good textural property after thermal aging.

Acknowledgement

This research was funded by a national project granted from the Ministry of Commerce, Industry and Energy, and Ministry of Science and Technology (1995–1998) and partially supported by the Brain Korea 21 Project.

References

[1] J.C. Summers, W.B. Williamson and M.G. Henk, SAE paper 880 281 (1988).

[2] J.C. Summers and W.B. Williamson, in: *Environmental Catalysis*, ACS Symp. Ser., Vol. 552, ed. J.N. Armor (Am. Chem. Soc., Washington, DC, 1994) p. 94.

[3] K.C. Taylor, in: *Catalysis: Science and Technology*, Vol. 52, eds. J.R. Anderson and M. Boudart (Springer, Berlin, 1984) p. 119.

[4] H. Muraki, H. Shinjoh, H. Sobukawa, K. Yokota and Y. Fujitani, Ind. Eng. Chem. Prod. Res. Dev. 25 (1986) 202.

[5] M. Skoglundh, H. Johansson, L. Lowendahl, K. Jansson, L. Dahl and B. Hirschauer, Appl. Catal. B 7 (1996) 299.

[6] A. Lemaire, J. Massardier, H. Praliaud, G. Mabilon and M. Prigent, Stud. Surf. Sci. Catal. 96 (1995) 97.

[7] J. Noh, O-B. Yang, D.H. Kim and S.I. Woo, Catal. Today 53 (1999) 575.

[8] D.H. Kim, S.I. Woo, J. Noh and O-B. Yang, Appl. Catal. A, in press.

[9] R. Craciun and N. Dulamita, Catal. Lett. 46 (1997) 229.

[10] T.E. Hoost and K. Otto, Appl. Catal. A 92 (1992) 39.

[11] A. Trovarelli, Catal. Rev. Sci. Eng. 38 (1996) 439.

[12] B.I. Whittington, C.J. Jiang and D.L. Trimm. Catal. Today 26 (1995) 41.

[13] A.F. Diwell, R.R. Rayaram, H.A. Shaw and T.J. Truex, Stud. Surf. Sci. Catal. 71 (1991) 139.

[14] H.S. Gandhi and M. Shelef, Stud. Surf. Sci. Catal. 30 (1987) 199.

[15] B. Harrison, A.F. Diwell and C. Halett, Platinum Metals Rev. 32 (1988) 73.

[16] M. Ozawa and M. Kimura, J. Mater. Sci. Lett. 9 (1990) 291.

[17] J.Z. Shyu, W.H. Weber and H.S. Gandhi, J. Phys. Chem. 92 (1988) 4964.

[18] G.W. Graham, P.J. Schmitz, R.K. Usmen and R.W. McCabe, Catal. Lett. 17 (1993) 175.

[19] M. Shelef, L.P. Haack, R.E. Soltis, J.E. deVries and E.M. Logothetis, J. Catal. 137 (1992) 114.

[20] L.P. Haack, J.E. deVries, K. Otto and M.S. Chatta, Appl. Catal. A 82 (1992) 199.

[21] C. Micheaud, P. Marecot, M. Guerin and J. Barbier, Appl. Catal. A 171 (1998) 229.

[22] P. Araya, C. Ferrada and J. Cortes, Catal. Lett. 35 (1995) 175.

[23] T.H. Fleisch, R.H. Hicks and A.T. Bell, J. Catal. 87 (1984) 398.

[24] J.F. Moulder, U.F. Stickle, P.E. Sobol and K.D. Bomden, in: *Handbook of X-ray Photoelectron Spectroscopy* (Perkin–Elmer, Eden Prairie, MN, 1992).

[25] M. Bettman, R.E. Chase, K. Otto and W.H. Weber, J. Catal. 117 (1989) 447.

[26] B.H. Engler, D. Lindner, E.S. Lox, A. Schafer-Sindlinger and K. Ostgathe, Stud. Surf. Sci. Catal. 96 (1995) 441.

[27] C. Hardcare, R.M. Ormerod and R.M. Lambert, J. Phys. Chem. 98 (1994) 10901.
[28] T. Miki, T. Ogawa, M. Haneda, N. Karuta, A. Ueno, S. Tateishi, S. Masuura and M. Sato, J. Phys. Chem. 94 (1990) 6464.
[29] K. Otto, L.P. Haack and J.E. deVries, Appl. Catal. B 1 (1992) 1.
[30] K.S. Kim, A.F. Gossmann and N. Winograd, Anal. Chem. 46 (1974) 197.
[31] R.J. Farrauto and M.C. Hobson, Appl. Catal. A 81 (1992) 227.
[32] Z. Karpinski, Adv. Catal. 37 (1990) 45.
[33] R.H. Hicks, Q.-J. Yen and A.T. Bell, J. Catal. 89 (1984) 498.
[34] M.J. Capitan, M.A. Centeno, P. Malet, I. Carrizosa, J.A. Odriozola, A. Marquez and J. Fernandez Sanz, J. Phys. Chem. 99 (1995) 4655.
[35] H.S. So, O-B. Yang, D.H. Kim and S.I. Woo, Stud. Surf. Sci. Catal. 130 (2000) 1379.